2016

X-ray protection, surface chemistry and rheology of ball-milled submicron Gd2O3 aqueous suspension

Ly B. T. La
Edith Cowan University, lbtly@ctuet.edu.vn

Yee-Kwong Leong

Christopher Leatherday

Pek I. Au

Kevin Hayward
Edith Cowan University, kevin.hayward@ecu.edu.au

See next page for additional authors

10.1016/j.colsurfa.2016.04.058

Edith Cowan University

Copyright Warning

CHAPTER 4: X-RAY PROTECTION, SURFACECHEMISTRY AND RHEOLOGY OF BALL-MILLED SUBMICRON Gd_2O_3 AQUEOUS SUSPENSION

Chapter 4 has been published as:

La, L. B. T., Leong, Y.-K., Leatherday, C., Au, P. I., Hayward, K. J., & Zhang, L.-C. (2016). X-ray protection, surface chemistry and rheology of ball-milled submicron Gd2O3 aqueous suspension. *Colloids and Surfaces A: Physicochemical and Engineering Aspects, 501(Supplement C)*, 75-82. doi: 10.1016/j.colsurfa.2016.04.058

CHAPTER 4: X-RAY PROTECTION, SURFACECHEMISTRY AND RHEOLOGY OF BALL-MILLED SUBMICRON Gd_2O_3 AQUEOUS SUSPENSION

4.1. Introduction

This study provides new insights into the potential for a non-lead-based material, gadolinium oxides (Gd_2O_3), compliance with an inexpensive and effective preparation method. Because of their high degree of penetration and toxicity, gamma and X-rays are used in a regimented environment to protect people from accumulative exposure, particularly in healthcare and research applications. To reduce radiation exposure risk from primary and incident X-ray beams to a safe level, interventional radiology physicians, patients, researchers and workers are required to wear customized personal protection garments and aprons during diagnostic imaging in hospital, clinic and dental facilities, X-ray scanning for airport security and other X-ray related applications [53]. Radiation protection has typically relied on commercial lead-based materials because of the high atomic number Z (82) and a high K-edge energy (88 keV) of the element (Pb). Unfortunately, Pb and its compounds are classified as poisonous substances for human health and the environment [58]. Indeed, while acute Pb toxicity can cause stomach pain, muscular spasms, nausea and vomiting, chronic exposure can result in high blood pressure, kidney problems and cancer [168]. Recent studies have shown that thermal neutron-cross-section parameters are also influential for attenuation of nuclear radiation [53,58]. Although the Z (64) and K shell energy (50.2 keV) indicators of the element gadolinium (Gd) are slightly lower than for Pb, its thermal neutron-cross-section is much higher than for Pb and most other elements. The neutron capture indicator of Gd is 254000±815 barns whereas that of Pb is only 0.661±0.070 barns [65]. Along with their nontoxicity, Gd and its compounds may be the most promising of non-Pb based radio-protective substances [31]. Additionally, the density of gadolinium (Gd) element shows lower density (7.9g/cm^3) than other potential radiation attenuation non-Pb based materials such as Bismuth (Bi) (9.75g/cm^3) and Tungsten (W) (19.3g/cm^3) [53]. This reduces the weight of radiation attenuation garments and increases user comfort.

Recently, several researchers and manufacturers have trialed hybrid composites that integrate Gd compounds for radiation shielding purposes. Fine Gd compound particles in micron and submicron- sized Gd particles are embedded into a dispersed phase of a polymer, for example, rubber or epoxy to minimize the weight and optimize geometric structure. This homogeneous dispersion of two components of such hybrid materials should not only increase human comfort and economic efficiency but also enhance functionality and

durability [53,55,57,169]. Liu et al., firstly developed a composite of gadolinium acrylate/natural rubber in which gadolinium acrylate ($Gd(AA)_3$) powder (>20μm) was synthesised by using an in-situ method [57].However, large particle size (>20μm) of $Gd(AA)_3$ reduced composite's potential medical X-ray shielding function. Ma et al., and Wang et al., dispersed commercial micro- and submicron-Gd_2O_3 powder in epoxy and poly ether ether ketone (PEEK), respectively [7,170]. In those suspensions with higher amounts of Gd_2O_3 (ϕ_s>0.017), the matrix was prone to cracking and tearing which inhibited the comprehensive investigation of the relationship between the Gd powder content and the shielding capacity of hybrid composites [7,57,170]. Lack of control in dispersing Gd particles in an uncured matrix can cause flocculation, agglomeration and sedimentation of powder which compromised the mechanical and functional properties of the final hybrid products in most other relevant studies [7,57,170]. Moreover, those studies did not evaluated real X-ray attenuating performance per unit weight of the hybrid materials.

In this work, stable colloidal gadolinium oxide (Gd_2O_3) aqueous suspensions were prepared and tested for radiation shielding performance. Their attenuation performance was investigated by X-ray absorbability in the keV energy ranges employed in diagnostic imaging in hospitals. In contrast to other studies which used available commercial Gd powder for radiation attenuation, submicron particles were synthesized from cheap precursor particles using high energy ball milling in the presence of NaCl. This milling strategy has been reported to be a cost effective and convenient process for different types of materials [148-152]. The large surface-area to volume ratios of the nano- or submicron-sized particles not only enhance photon absorption but also facilitate homogeneous dispersion of the powder phase to create a durable hybrid network structure [171]. Next, surface chemistry and rheology of resultant submicron Gd_2O_3 aqueous suspensions were studied using the yield stress and zeta potential techniques. This information can be used to minimize agglomeration and coalescence of Gd_2O_3 powder in the mixing procedure, consequently increasing the material's radiation absorption [2]. Then, the X-ray radio-protective effectiveness, in the range of interventional radiology (50-100kVp) of Gd_2O_3 aqueous suspensions in different solid concentrations was evaluated and modeled. Finally, the effective weight per thickness of material of Gd_2O_3 suspensions was compared with commercial lead-based and other conventional radiation attenuation materials at the same effective radiation attenuation needed for practical applications. This research is significant for developing a non-lead-based

material, Gd_2O_3 suspension, which offers effective radiation attenuation with weight-thickness minimization and safe use and disposal.

4.2. Materials and methods

4.2.1. Submicron-sized Gd_2O_3 particles/water slurry preparation

Precursor gadolinium (III) oxide (Gd_2O_3) powder with a purity of 99.99%, size distribution of d_{10}=0.28µm, d_{50}=4.34µm and d_{90}=10.6µm, and particle density of 7.407g/cm^3, was purchased from Alfa Aesar (United Kingdom). A high energy SPEX8000 mixer/mill, using hardened steel balls (12.5 mm diameter) at ambient temperature, was used for producing submicron particles. A fixed ball-to-Gd_2O_3 powder weight ratio of 7:1 was adopted with and without sodium chloride crystals (NaCl) (99%; supplied by Aldrich Sigma) at Gd_2O_3-to-NaCl weight ratios of 1:1, 1:1.5 and 1:2. These mixtures were ground at 10, 20, 30, 40, 50, 60, 70, 120 and 130 minutes. Subsequently, the NaCl was removed and the Gd_2O_3 particle size distribution determined. To remove the NaCl, the milled Gd_2O_3/NaCl mixture was dissolved in distilled water at a weight ratio of 1:10, stirred continuously for 10 minutes and left for 6 hours until all particles had settled to the bottom of a 2000ml beaker. The upper water layer was removed and its pH and electric conductivity were measured. This sediment was again diluted with demonized water in an ultrasonic bath and the pH was adjusted to about 11 by adding sodium hydroxide (NaOH) (99%; from Aldrich Sigma). The use of mild alkaline condition with the addition of NaOH was aimed to remove adsorbed impurities on the particle surfaces[172]. The washing procedure was conducted repeatedly until the conductivity of the upper water layer of slurry was less than $5x10^{-4}$ S/cm which is equivalent to a concentration of ~0.005 M NaCl[172].This pristine Gd_2O_3 aqueous suspension was sonicated by a Branson sonifier at 70% amplitude for one minute to improve the dispersion of the milled particles. A small amount of samples was collected and used in the size distribution determination using a Malvern Mastersizer Microplus Particle Size Analyzer. The morphology of milled Gd_2O_3 particles were characterized by a Zeiss 1555 VPSEM.

4.2.2. Surface chemistry and rheology of the Gd_2O_3 slurry

Centrifugation at 2000 rpm for 5 minutes (Sigma 2-6, Germany) separated the concentrated Gd_2O_3 material from the diluted washed slurry. The solid concentration of this slurry was determined by evaporating of a small sample (2 g) of the slurry in an oven for 5 hours at 120^{o}C. The appropriate amounts of distilled water were then added to the thick suspension to prepare the slurries at different solid volume fractions; 0.0023 for zeta

potential-pH characterization, and 0.23 to 0.34 for yield stress-pH. All suspensions were again sonicated for one minute at 70% amplitude using the sonifier. The zeta potential-pH behaviour was characterized using a Colloidal Dynamic ZetaProbe operated in the potentiometric titration mode using 0.7 M KOH or 0.7 M HNO_3 solutions as the titrants. The (static) yield stress-pH behaviour was characterized using a Brookfield vane viscometer. At each step change of pH, the sample was agitated vigorously with a spatula for at least 15 minutes before pH and yield stress were measured. The maximum torque applied on a rotating (0.4 rpm) vane submerged in the colloid was transformed to the corresponding yield stress [173].

4.2.3.X-ray shielding properties

Gd_2O_3 aqueous suspensions (25ml) at different solid volume fractions (ϕ_s) of 0.0071, 0.015, 0.032, 0.055, and 0.082 at pH of 8.8 were prepared. The pH adjustment was done using HNO_3 to reduce coalescence and agglomeration of submicron Gd_2O_3 particles in the slurry. These suspensions were contained in 5×5 cm cell culture flasks which created a 10 mm constant thickness sheet of suspension. A blank sample (an empty cell culture flask) and a zero sample (a flask with 25ml of de-ionised water) were used for calibration. The attenuation capacity of these slurries was tested at Royal Perth Hospital with beams of six different energies from 50 to 100kVp, the common diagnostic radiographic region. The photon beams from an X-ray tube source of a Mobile DR X-ray unit (GE Optima XR220AMX) were emitted for 25 seconds at a current of 100 mA to suspensions as a radiation shielding screen. Radiation transmitted through samples was collected, recorded and analysed using a free air chamber of Non-invasive X-ray Beam Analyser (Unfors Xi R/F & MAM). In this study, the broad beam geometry of a DIN 6857 Standard test method was used in which the distance from focal spot to chamber was one metre, and the sample sheets were located directly in front of this indicator. This geometry generates a more accurate attenuation measure because it is based on the total radiation reaching the chamber (contributed by penetrating primary and scattered radiation through materials), and the fluorescence generated by the sample itself [10,70].

4.3. Results and discussion

4.3.1. Size distribution and morphology of synthesized Gadolinium oxide powder

If a milling additive was not used, the soft waxy Gd_2O_3 particles adhered together and to the milling vessel in the first 4 minutes of grinding. These problems were overcome by

adding NaCl (99%; Aldrich Sigma) which also helps create a more abrasive environment [160,161]. Additionally, the presence of NaCl kept the milled particles apart thus prevents them from re-welding or sintering during grinding [160,161]. The specific advantages of using NaCl in aiding the milling and producing submicron Gd_2O_3 include its low cost and being non-toxic, brittle, inert and water-soluble[160,161]. The median size and size variation of milled Gd_2O_3 particles after the ball milling time are influenced by the milling time, and the quantity of NaCl will be added. The measured values of d_{10}, d_{50} and d_{90} indicate the values of the particle diameter (μm) in the cumulative distribution at 10 vol.%, 50 vol.% and 90 vol.%, respectively.In general, while a d_{50} value characterizes the median size of particles, d_{10} and d_{90}values represent their cumulative size distribution. The resulting data show that d_{10} values, of initial and crushed Gd_2O_3 powder at different milling times and with different Gd_2O_3: NaCl ratios, were similar (about 0.26μm). Meanwhile, the median diameter of all samples at d_{50} dramatically decreased from 4.34μm for the original Gd_2O_3 to around 0.38μm in the first 10 minutes grinding and stablised in the subsequent milling time intervals. The value from d_{90} values were strongly affected by Gd_2O_3: NaCl weight ratios (1:1, 1:1.5 and 1:2).

Figure4.1A shows the resulting Gd_2O_3 particle size curves after milling with different amounts of NaCl at d_{90}. It shows that at a weight ratio of 1.5:1 of NaCl: Gd_2O_3 the resultant d_{90} is less than 0.8μm after 70 minutes milling. This means that 90 vol.% Gd_2O_3 particles has a size of less than 0.8μm. For longer milling time of 130 minutes, the d_{90} was found to increase slightly for all samples with different NaCl: Gd_2O_3 ratio due to the aggregation of crushed fine particles as a result of their large specific electrostatic surface area [156].

Figure4.1Bgives comparable statistical size distribution patterns of the 70 minutes-milled powder at the ratios 1:1, 1:1.5 and 1:2 of Gd_2O_3: NaCl. Two main peaks of volume percentage of particle are found in the diameter ranges of less than 1μm and more than 1μm. Producing fine particles less than 1μm (submicron) was the expected outcome of this research. The ball milling moves the peaks of all samples from the range of more than 1μm to less than 1μm size. However, only the peak of Gd_2O_3 powder at the ratio of 1:1.5 reaches the highest volume in the range of 0.14-1μm, and the lowest and narrowest peak in the range of more than 1μm.Then, the submicron Gd_2O_3 particles with d_{10}, $d_{50,}$ and d_{90} values of 0.23, 0.38, 0.8μm respectively which had been milled for 70 minutes with NaCl (at a weight ratio 1:1.5 of Gd_2O_3: NaCl) were used for the next stage.

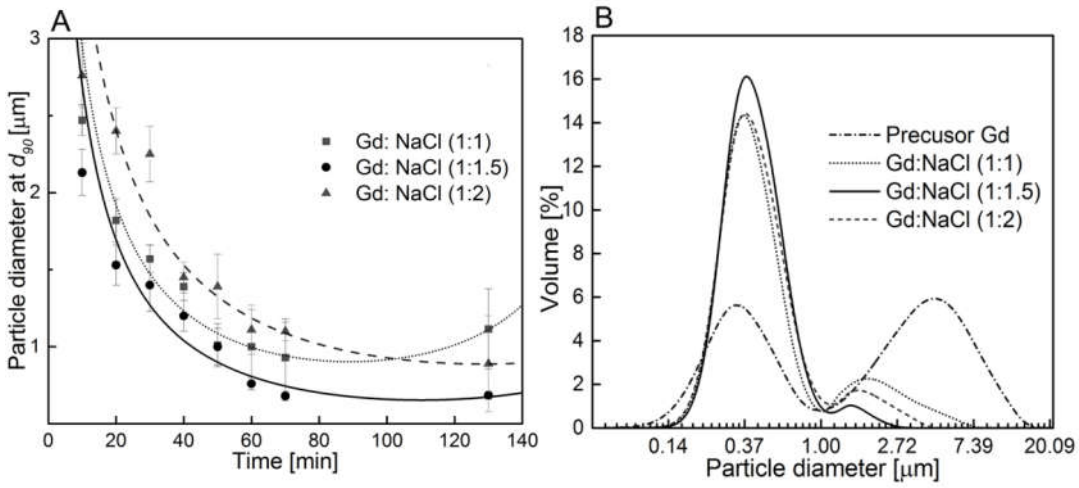

Figure 4.1. (A) The particle diameter of gadolinium oxide versus milling time at different ratios of Gd_2O_3:NaCl at d_{90}, and (B) The size distribution of gadolinium oxide for 70 minutes of milling at different Gd_2O_3:NaCl ratios.

The SEM image (Figure4.2 A-B) provides information on the morphology and sizes of premilled and milled Gd_2O_3. The ball mill process generated a submicron-spherical and -cylindrical Gd_2O_3 powder from micron precursor. Although a common consolidation process is considered to be the simplest, highest yielding and most cost-effective approach for mass production of a variety of submicron-grained metallic compounds, synthesis of submicron crystalline Gd_2O_3 powder has rarely been undertaken controlling the size of Gd_2O_3 crystal is difficult [171]. The typical ball milling procedure was employed for synthesis of nano- and submicron- Gd_2O_3 particles that was induced by the reaction of gadolinium chloride ($GdCl_3$) and sodium hydroxide (NaOH) or calcium oxide (CaO); however, this mechano-chemical approach produced many by-products [158,159]. In contrast, this research used NaCl as an inert additive to facilitate the size reduction mechanically during the ball milling process; therefore, a high yield and purity of submicron-sized Gd_2O_3 powder could be achieved.

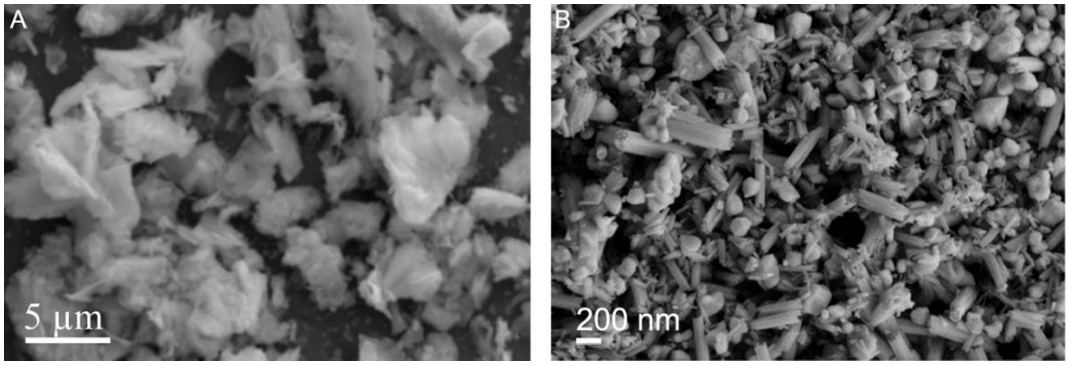

Figure 4.2. SEM micrograph of premilled (A) and milled Gd_2O_3 (B) obtained after 70 minutes of milling at a weight ratio of 1:1.5 of Gd_2O_3: NaCl

4.3.2. Surface chemistry and rheology of resulting submicron-sized Gd_2O_3 aqueous suspensions

In the absence of surfactants, external magnetic and electric fields, the yield stress, flow behaviour, and sedimentation performances of a colloidal suspension were determined by interaction between the van der Waals attractive and electrostatic repulsive forces [174-178]. While the magnitude of zeta potential characterises the strength of the repulsive force, the value of yield stress represents the strength of attractive interaction between particles [172,178]. A zeta potential with a large magnitude indicates that the net particle interaction is repulsive and the suspension is dispersed. A low zeta potential denotes a net attractive interaction between particles dominated by the van der Waals force and the suspension is flocculated with a yield stress. The smaller the zeta potential the larger is the yield stress [179]. Thus, the zeta potential- and yield stress-pH can be used for predicting the Gd_2O_3 particle behaviour in suspension and identifying the dominant surface force operating and the key factors that affect it. Accordingly, effective control of the dispersion-flocculation performance of Gd_2O_3 aqueous slurries is possible, and can generate stable Gd_2O_3 colloidal dispersion. NaCl in solution functions as an indifferent electrolyte and provides the ionic concentration that determines the thickness of the electric double layer. Other 1:1 salts such as KCl and KNO_3 also provide similar function [172]. The thickness of the double layer and surface charge density determine the strength of the interparticle repulsion interaction and the stability of the suspension. The removal of adsorbed anionic impurities at mild alkaline condition during the washing process increases the positive charge density of particles at pH below the point of zero charge [172,180-182]. The low conductivity or salt concentration

(~0.005M NaCl) after washing indicates the double layer is quite thick and stabilise the particles with high positive or negative charge density in the suspension by repulsive force

Figure 4.3 shows the influence of pH on the zeta potential for the resulting Gd_2O_3 aqueous suspension (ϕ_s =0.023, d_{50}=0.38μm) at a conductivity of 4×10^{-5}S/cm. The isoelectric point (IEP) or positive to negative charge reversal of Gd_2O_3 aqueous suspension occurs at a distinctive high pH of 10.88 compared with other inorganic compounds such as Titanate (pH =4), TiO_2 (pH =7), γ-Al_2O_3 (pH =9.8), ZrO_2 (pH=6.5) [172,178,179,183-185]. This point of zero zeta potential indicates the absence of electrostatic repulsive force with only the van der Waals force operating in the suspension. The positive and negative charge branches of the zeta potential curves are not balanced. Indeed, while the zeta potential increases strongly in the positive charge region with decreasing pH, the magnitude of the zeta potential in the negative region shows a slight increase as pH rises.

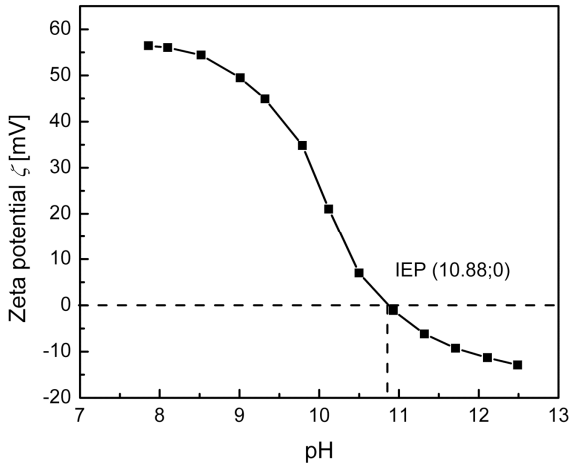

Figure 4.3 The zetapotential (ζ) -pH behaviour of a milled and cleaned Gd_2O_3 suspension

The flocculated state of different weight solid concentrations of Gd_2O_3 slurry was determined to span from a pH of 8.5 to 12.5 via the yield stress behaviour (Figure 4.4). The plots also show a zero yield stress that characterises the completely dispersed state of the Gd_2O_3 aqueous suspension for a pH less than 9. The result is consistent with the high positive zeta potential that is sufficient to electrostatically stabilise the dispersion. The maximum stress (τ_{ymax}) of the different solid concentration Gd_2O_3 suspensions was observed at a pH of about 11, thus agreeing with the pH for the isoelectric point. This maximum yield stress increases sharply with solid fraction concentration. Indeed, while the maximum yield stress of suspension (ϕ_s=0.23) is nearly 39 Pa, that of suspension (ϕ_s=0.34) is 500 Pa, nearly thirteen-fold greater. Here only the attractive force (van de Waal force) is present [183].

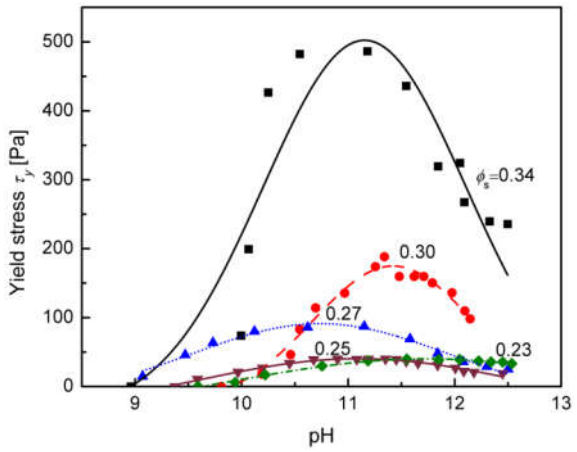

Figure 4.4. The influence of solid volume fraction (ϕ_s) on the yield stress-pH of Gd_2O_3 aqueous suspensions

Figure 4.5 presents the influence of volume fractions (ϕ_s) in the range of 0.23 to 0.34 of Gd_2O_3 suspension (d_{50}=0.38µm) on the maximum yield stress. The log-linear plot displays a linear relationship which is described by a power law model in Equation 6.

$$\tau_{y_{max}} = 1.34 \cdot 10^6 \phi_s^{7.33} \tag{4.1}$$

The slope has an unusually high value of 7.33 while the values for most other oxide suspensions are in the range 3-4 [183]. Such a high value shows an extremely sensitive dependence of maximum yield stress on the solid volume fraction of the Gd_2O_3 aqueous slurry. The maximum yield stress is also strongly influenced by the solid volume fraction, size, shape and nature of the particles [183]. For similar size and volume fraction values, a ZrO_2 slurry (d_{50}~0.25µm; ϕ_s= 0.18) exhibits a maximum yield stress of 440 Pa, while for a comparable Gd_2O_3 slurry (d_{50}~0.38µm; ϕ_s= 0.23), it is only 39 Pa[183]. This means the flocculation behaviour of Gd_2O_3 particles in water strongly depends on physical properties such as the shape and the nature of the particles as represented by the Hamaker constant[186]. The geometry of the particle-particle interactions in this suspension is very complex due to the large variation in the shape of milled Gd_2O_3 particles (Figure 4.2). The van der Waals attraction comprises interaction between; cylinders, spheres and cylinders, and spheres in cross and parallel configurations. This may be responsible for the high exponent value.

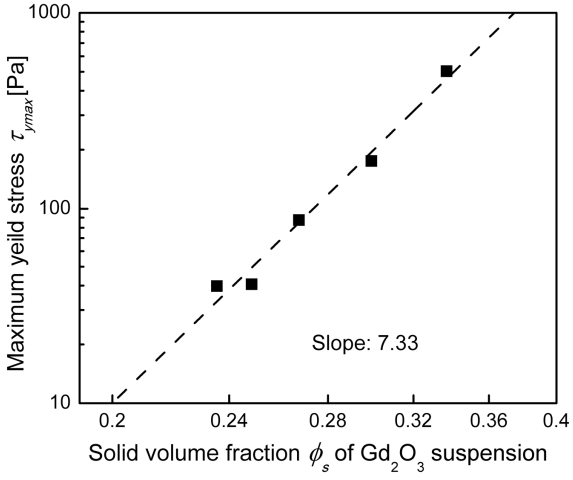

Figure 4.5. The relationship of maximum yield stress ($\tau_{y,max}$) and solid volume fraction (ϕ_s) of Gd_2O_3 suspension in log-log scale

Most oxide suspensions obey the Derjaguin, Landau, Vervey, and Overbeek (DLVO) theory via the yield stress-DLVO model. The yield stress (τ_y)is related to zeta potential (ζ)via the following equation 4.2[172,175,187]:

$$\tau_y \approx \frac{\phi_s^2}{a}\cdot\left(\frac{A_{121}}{12\cdot D_o^2} - 2\cdot\pi\cdot\varepsilon_w\cdot\zeta^2\frac{\kappa\cdot e^{-\kappa\cdot D_O}}{(1+e^{-\kappa\cdot D_O})}\right) \tag{4.2}$$

At the point of flocculated-dispersed transition where yield stress is zero, the Hamaker constant of Gd_2O_3 suspension is calculated from the magnitude of zeta potentials (ζ_{crit}) as follows[172,175,187]:

$$A_{121} = \frac{24\cdot D_o^2\cdot\pi\cdot\varepsilon_w\cdot\kappa\cdot e^{-\kappa\cdot D_O}\cdot\zeta_{crit}^{\ 2}}{(1+e^{-\kappa\cdot D_O})} \tag{4.3}$$

Equation 4.3shows a function of the Hamaker constant (A_{121}) which depends on critical zeta potential (ζ_{crit}); D_o, a,$\varepsilon_w$and κ are constants which are the surface distance between two particles, particle radius, permittivity of water and Debye parameter, respectively.

Figure 4.6reveals that a decrease of the yield stress linearly increases the square of the zeta potential (τ_y-ζ^2)of Gd_2O_3 dispersion. This result demonstrates that gadolinium oxide slurry dispersed-flocculated behaviour satisfied the DLVO theory [172]. The plot τ_y-ζ^2in the positive charged region was used to determine the critical zeta potential because a zero yield stress of all Gd_2O_3 aqueous slurries was observed there [188]. Extrapolating the linear plot τ_y-ζ^2 to zero yield stress, the intercept value is 2520 mV^2 and the critical zeta potential (ζ_{crit})is equal to 50

mV. The magnitude of this potential characterises the strength of the repulsive force which is equal to van der Waals attractive force at the dispersed-flocculated transition point. With a similar median size to Gd_2O_3, a TiO_2 dispersion (d_{50}~0.68μm) had a very similar magnitude of critical zeta potential (49mV) to that of Gd_2O_3 suspension (d_{50}~0.38μm) (50 mV). From equation 4.3the Hamaker constant of Gd_2O_3 in an aqueous suspension is predicted to be similar to the A_{121}(68 zj) value for TiO_2 as determined by this method [187].

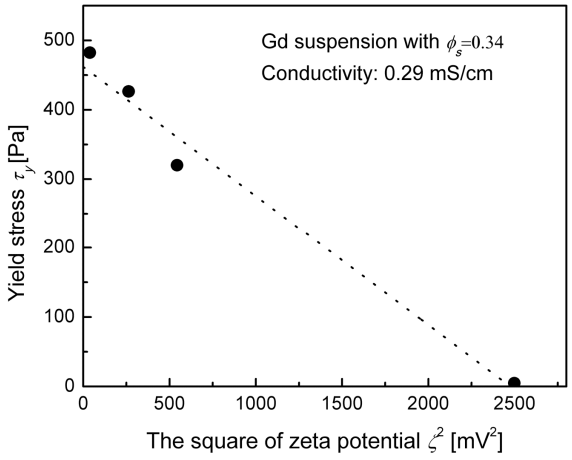

Figure 4.6. The correlation between yield stress (τ_y) and the square of zeta potential (ζ^2)

4.3.3. Radiation shielding properties of Gd_2O_3 suspension fractions

Six suspension samples with different volume fractions of Gd_2O_3 ranging from 0.0071 to 0.082 at a pH near dispersed-flocculated transition (pH~8.8) were used to test X-ray radiation attenuation. While factors which directly affect the radiographic density of X-ray beams such as tube current, and exposure time and distance from source remained unchanged, the intensity of the penetrating range of X-ray radiation was changed by increasing the applied voltage in a stepwise manner by 10 kilovolts (kVp) from 50 to 100kVp of tube voltage [189]. It should be noted that the penetrating capacity of X-ray beams depends on their energy. The higher the energy of the X-ray photon, the greater its penetration and the lower is the X-ray attenuation of the material. The kilovoltage applied across the X-ray tube is the maximal energy (keV) lying on a continuous energy spectrum of the resultant photon collected by chamber. The absorbability of the photon ray for a given material relies principally on the thickness of the absorber and the energy of the beam. The dose unit gray (Gy) is used to describe the quantity of energy captured per unit mass of the material [190].

Figure 4.7A shows an increase in effective transmission with an increased level of energy for the same volume fraction of the suspensions. A linear relationship between log transmittance coefficient (T) and a volume fraction (ϕ_s) is observed at different levels of photon energy. Therefore, their relationship can be described by the equation below:

$$T = k \cdot e^{-B\phi_s} \quad (4.4)$$

with ($0 \leq \phi_s \leq 1$) and ($0 \leq T \leq 1$)

$$T = e^{I}$$

where T is the transmitted fraction, through a suspension, which is a ratio between dose through a specimen and dose through an empty culture flask (blank sample); the corresponding attenuation capacity is (1-T); B is the absolute value of the slope, k is a constant and I is the intercept of linear regressions of ln(T)-ϕ_s at different energy levels. The negative values of all slopes show an inverse dependence of penetrative capacity of suspensions (T) on the volume fraction (ϕ_s). Transmittance coefficient of 100kVp at the same volume fraction shows higher values than that of other kVp. Accordingly, in six energy quality photon beams, X-rays at an energy level of 100kVp are the most difficult beams to shield. A mathematical equation describing the relationship between transmittance coefficient (T) and a volume fraction (ϕ_s) at 100kVp is given below:

$$T = 0.756 \cdot e^{-34\phi_s} \quad (4.5)$$

The X-ray shielding property of a material is measured by its capacity to absorb high-energy photon beams. A low level of absorbability allows penetration of these incident waves negatively affecting internal and external human body organs. Figure 4.7B presents a linear reduction of the attenuating capacity or X-ray absorbability of Gd_2O_3 slurry versus an increases the energy level at the same volume fraction with the slopes ranging from 0.12 to 0.23 [10,53,58]. The result also shows that pure water with a thickness of 1cm can also absorb 17% energy of 100kVp and 23% of 50kVp with a slope of 0.05. Adding an amount of Gd_2O_3 to create a particle dispersion with ϕ_s~0.0071 at the same thickness, can improve the effective radiation attenuation by nearly 2.2 times. Similarly, an increase in volume fractions of Gd_2O_3 suspensions from 0.015 to 0.082 significantly increases the X-ray shielding capacity. Specifically, a Gd_2O_3 suspension with ϕ_s~0.082 can attenuate or absorb > 95% of X-ray intensity (or ≤5% transmission) at all energy levels in the range of 50-100kVp. It satisfied

the requirement for a standard comparison to investigate of an alternative materials to equivalent Pb-based garments for radiation protection [10].

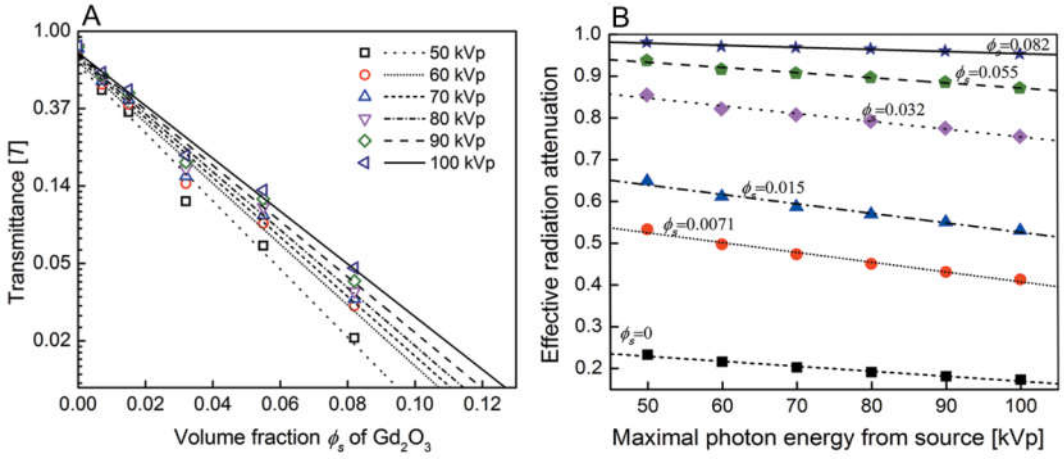

Figure 4.7 (A) Logarithmic transmittance coefficient (T) for different volume fraction values (ϕ_s) of Gd_2O_3 suspensions in different X-ray energy and (B) The plot of effective radiation attenuation and maximal photon energy from the source (kVp).

In addition to radiation shielding effectiveness, minimisation of the weight per unit thickness of radiation-protective garments is an important consideration. To directly compare the weight versus equivalent shielding capabilities of radiation attenuation elements, thickness parameters (cm) of Gd_2O_3 suspensions and conventional radiation protection materials were converted to their corresponding weight per area unit (g/cm^2) [10,53]. X-rays at an energy level of 100kVp were the most difficult to shield in this study. Consequently, the converted weight per thickness measurements at equivalent attenuation effectiveness of Gd_2O_3 (ϕ_s~0.082) are compared with that of pure Pb, commercial Pb-based material, concrete, steel, glass and wood at this energy level [53,55].

Table4.1 shows a comparison of weight-thickness (g/cm^2) between Gd_2O_3 suspension in volume fraction (ϕ_s~0.082) and other materials of similar effective transmission or attenuation capacity. The weight-thickness measurement of dispersed Gd_2O_3 aqueous is more than 5-fold, 1.4-fold, 7-fold and 16-fold lower than that of equivalent concrete, steel, glass and wood materials, respectively. The estimated weight-thickness of Gd_2O_3 powder per square centimetre of suspension is 0.6 g, which is approximately equivalent 0.5 mm Pb is 0.57g [68]. It should be noted that pure Pb is never used in practical X-ray protection because of its toxicity [10,53]. The Gd_2O_3 suspension shows a total value of 1.5 in g/cm^2 measurement ($0.6g/cm^2$ Gd_2O_3+ $0.9g/cm^2$ H_2O) compared to a commercial Pb-based apron with value

>1g/cm^{2}depending on the kind of polymer matrix [53,191]. As a result, a non toxic Gd_2O_3 suspension synthesised in this research provides potentially X-ray valuable attenuation per unit mass and volume.

Table 4.1. The comparison of weight-thickness (g/cm^2) of Gd_2O_3 suspension (ϕ_s~0.082) and other commercial X-ray protective materials at the equivalent effective attenuation capacity.

	Thickness (cm)	Density (g/cm^3)	Weight- thickness (g/cm^2)	Reference
Gd_2O_3 suspension (ϕ_s ~0.082)	1	7.4 1	0.6 (Gd_2O_3) 0.9 (H_2O)	-
Pb Equivalent	0.05	11.34	0.57	[53,68]
Commercial Pb-based apron Equivalent	-	-	≥1	[10,68,191]
Concrete Equivalent	3.36	2.4	8.1	[68,192]
Steel Equivalent	0.26	7.8	2.1	[68,193]
Plate Glass Equivalent	4.22	2.5	10.6	[68,194]
Wood Equivalent	38.41	0.64	24.6	[68,195]

4.4. Conclusion

The study provides essential information for developing an inexpensive and effective method, to produce non-lead-based radiation protection garments, based on a Gd_2O_3 suspension, for use in interventional radiology procedures or other X-ray related fields. This material offers promising X-ray radio-protective effectiveness per unit mass; and most importantly, its use and disposal are much safer than lead based materials. In this work, to optimize the radiation attenuation performance, very small particles of Gd_2O_3 were prepared and then dispersed uniformly as a slurry in water with appropriate pH. Firstly, submicron Gd_2O_3 particles with a size distribution of d_{10}~0.23, d_{50}~0.38 and d_{90} ~0.8μm were generated through a conventional and cost effective ball milling method over 70 minutes with the

mechanical support of a NaCl additive (1:1.5 Gd_2O_3:NaCl). The dispersed-flocculated behaviour of Gd_2O_3 and thus the uniformity of suspension were determined by pH and the solid volume fraction. Flocculation or domination of attractive particle force of Gd_2O_3 in an aqueous medium was investigated in the pH range from 9 to 12.5 in which maximum flocculation occurred at pH of 11. The point of dispersed-flocculated transition or balanced state of attractive and repulsive forces in the slurry, which determines the stable dispersion of Gd_2O_3 aqueous suspensions, was about pH 9. Flocculated performance of the given particles is also affected by solid volume fraction (ϕ_s) which strongly depends on its physical properties such as size, shape and nature of particles. Compared with other metals oxide of similar particle size, van der Waals attractive force of Gd_2O_3 particles in suspensions are unusually sensitive to the change of the volume fraction. This is due to the large variation in the shape and nature of the particles as characterizing by the Hamaker constant. Based on the above information, the uniformly dispersed Gd_2O_3 aqueous suspensions prepared in this work provided the highly effective X-ray radiation shielding performance required for a potential non-Pb based radiation attenuator. Our results are significant for the development of a superior alternative to lead-based radiation protective garments in interventional radiology procedures or other X-ray related fields.